J Mater Sci (2008) 43:1471–1479
DOI 10.1007/s10853-007-2325-z

An examination of effects of solidification parameters on permeability of a mushy zone in castings

Danylo B. Oryshchyn · Ömer N. Doğan

Received: 17 August 2007 / Accepted: 15 November 2007 / Published online: 12 December 2007

Abstract A model describing the development of dendritic structure and the resulting gradient of flow resistance to interdendritic liquid is presented. The Hagen–Pousielle version of D'Arcy's equation for flow through a porous structure is developed as a function of cooling rate and liquid volume fraction. Applied to finite elements in a unidirectionally cooled casting model, permeability gradient, feeding flow-rate required to prevent porosity, and mushy-zone liquid pressure drop at this flow rate are evaluated for the simple Fe–2Cr–0.5C and Al–5Cu castings exhibiting asymptotic and linear temperature profiles, respectively. The model shows permeability of the dendritic structure in the mushy zone dropping sharply, approaching the root of solidification front (solidus). Also shown is the effect of relative magnitude of primary and secondary arm spacing. If secondary dendrite arm spacing approaches primary arm spacing, the permeability for flow normal to primary dendrite arms approaches or even surpasses the permeability for flow parallel to primary dendrite arms.

Introduction

One theme of investigation into the causes of porosity in castings has focused on the friction-based resistance to flow of liquid through the mushy zone of a solidifying casting. Investigations of dendritic alloys have examined the microstructure of the casting, correlating this microstructure with resistance to flow by applying D'Arcy's equation [1], and Hagen–Poisueille flow [2]. The Kozeny–Carmen relationship [3] is also applied for equiaxed dendritic structures. Experiments have been performed to further the understanding of this structure/flow relationship. Streat and Weinberg [4] measured fluid flow through partially remelted lead–tin alloy comprising columnar or equiaxed dendritic structures. Streat and Weinberg applied the Hagen–Poisueille model of interdendritic flow (modeling the interdendritic channels as capillary tubes) with a tortuosity factor to account for the fact that these channels are not straight and are asymmetrical. "Tube diameter," here, was given by examining primary dendrite arm spacing. D'Arcy's law was shown to apply during initial flow for their experiments, but coarsening of the dendrites as flow continued in the remelted specimen broke the relationship between pre-experiment microstructure and flow resistance. Murakami et al. [5] modeled the flow normal to columnar dendrites in borneol-paraffin as laminar flow through interstices of slender, rectangular cross section. They showed permeability of this structure to be proportional to the square of primary dendrite-arm spacing and the cube of liquid fraction. Nielson, et al. [6] measured permeabilities of aluminum–copper alloys with equiaxed dendrites, validating the theoretical work of Wang et al. [7], and Kozeny–Carmen. Nasser-Rafi et al. [8] showed that secondary dendrite arm spacing did not affect flow parallel to primary dendrite arms. Santos and Melo [9] continued Streat and Weinberg's work [4] by refining expressions for channel cross-section and developing the tortuosity factor as a function of dendrite arm spacing and liquid volume fraction. Sabau and Viswanathan [10] combine the effect of predicted pore growth in the mushy zone with dendrite arm spacing to restrict demand for liquid flow and ease of flow, respectively.

D. B. Oryshchyn · Ö. N. Doğan (✉)
DOE National Energy Technology Laboratory, 1450 Queen Avenue, S.W, Albany, OR 97321, USA
e-mail: omer.dogan@netl.doe.gov

Relationships between the temperature history of the casting and the resulting microstructure have brought prediction of porosity even closer to foundry practice. Niyama et al. [11], correlated a ratio of temperature gradient to cooling rate with the occurrence of shrinkage porosity. They noted that the correlation does not explain the mechanism for shrinkage, but that the correlation has been predictive in laboratory and industrial scale steel castings. Flemings [12] demonstrated a relationship between cooling rate and dendrite arm spacing.

This work may be seen as a concatenation of the permeability/microstucture relationship developed by Santos and Melo [9] with the microstructure/cooling rate relationship developed by Flemings [12] and applied to finite elements of a casting geometry to develop a structural gradient throughout the mushy zone.

The permeability gradient model is D'Arcy's equation for fluid flow through porous media applied through finite elements to the mushy zone of a solidifying dendritic material. The target value for this model is the minimum necessary head pressure for casting that will prevent shrinkage-induced porosity. The algorithm used takes inputs of cooling rate and casting temperature profile and outputs a predicted permeability gradient and a necessary riser height to counteract the decreased permeability in the cooler parts of the mushy zone. Key to the development of riser height requirements from permeabilities is the volumetric flow rate of the liquid at the freezing front of the casting. The volumetric flow rate of solid (the "solid flow rate", i.e., volumetric solidification rate) is given by the cooling rate and temperature gradient associated with the portion of the mushy zone whose complete solidification is imminent.

D'Arcy's equation for flow through porous media gives a simple, empirically derived, description of area-averaged flow resistance in these media. Minimizing the element size to which D'Arcy's equation is applied enables higher resolution of flow description than would its application only to the entire mushy zone. A finite element application of D'Arcy's equation allows the effect of the partially developed dendritic structure (toward the warmer end of the mushy zone) to be evaluated and included in the overall resistance to liquid flow associated with the freezing front of the casting. Finally, the goal of this method is to allow porosity prediction to be made, essentially, from information about the temperature profile, alloy composition, and cooling rate of the casting.

The model at this stage is uniaxial and uses a particular solution of the differential equation for heat transfer during phase-change. Further iterations of the model will develop the temperature profile in two and then three dimensions.

Two parameters, permeability and minimum necessary interdendritic liquid flow rate, are developed to predict the minimum required head pressure for producing a casting in which shrinkage-caused porosity does not occur. Permeability throughout the mushy zone is a function of the cooling rate at the onset of dendrite development and the temperature-dependent liquid fractions extant throughout the mushy zone. Necessary flow rate is defined as the time required to fill the remaining liquid fraction volume in elements adjacent to the solidus. Cells that are modeled are those that are neither completely liquid nor solid. Thus, the time allowed in this model for this volume to be filled is the time taken by the coolest mushy cell to traverse from its current temperature to the solidus temperature (given the local cooling rate for that element).

Permeability gradient is developed as a function of temperature, cooling rate, and liquid fraction. Assumptions of the formation mechanisms are:

- The casting is uniaxially cooled and the flow is assumed uniaxial.
- Unless a temperature gradient is given, the particular solution to the differential equation for temperature during the phase change in this casting scenario defines the temperature profile throughout the casting at any point in time.
- The temperature and microstructure of a given finite element is uniform.
- The scale of the element is sufficient that D'Arcy's area-averaged flow rate assumptions are valid. The length scale of the finite elements is at least one order of magnitude larger than dendrite arm spacing [13].
- Cooling rate at liquidus determines the dendrite arm spacing. It is assumed that nucleation takes place at the liquidus and the cooling rate at the liquidus determines the number of dendrites in a given volume element.
- Dendrite growth is considered through liquid volume fraction; however, dendrite coarsening due to chemical potential differences (Ostwald ripening effect) is ignored.
- Viscosity of the remaining liquid is constant.
- Capillary forces are ignored.
- For the time interval over which the root cell (closest to the solidus) freezes the dendritic structure throughout the mushy zone is considered static. Flow through this structure is examined to develop pressure requirements for feeding.

Permeability gradient model

This model surmises the formation of porosity voids in castings is a function of the ability of liquid to fill voids in the densest region of the mushy zone. This model does not consider contribution of dissolved gases to the porosity

formation. The voids in the mushy zone occur on shrinkage as the final interdendritic liquid freezes. A minimum volumetric flow rate of liquid must be achieved to fill these voids before final solidification of this liquid prevents flow. This minimum necessary flow rate is proportional to the progress, over time, of the freezing front as the casting solidifies—the "flow rate of solid". The proportionality constant is the ratio of the solid density of interdendritic composition to its liquid density. Adequate flow rate of liquid into the areas of the mushy zone closest to the final solidification front is possible only as long as the pressure driving it through the mushy zone matches or exceeds the pressure drop which would occur at the minimum necessary flow rate.

The pressure drop across the mushy zone is a function of the resistance to flow of the dendritic structure formed there. The dendrite packing density of this structure is not constant across the mushy zone, but increases as one approaches the final solidification front (solidus). Therefore, the resistance to flow of a given length of mushy zone varies with its position within the mushy zone. Regions closest to the solidus will offer the greatest resistance. However, the ability of liquid to flow is already attenuated by travel through upstream portions of the mushy zone before these most restricted regions are encountered. Taking this attenuation into account may allow more precise, accurate determination of predicted porosity, making possible closer optimization of casting parameters.

To take flow-pressure attenuation into account, the minimum necessary flow model examines flow of interdendritic liquid through a full gradient of permeabilities in the mushy zone. As shown in Fig. 1, the permeability of the dendritic regions of the mushy zone is smallest (hardest to penetrate) nearest the root of solidification front (solidus) of the casting. As the distance from this root increases

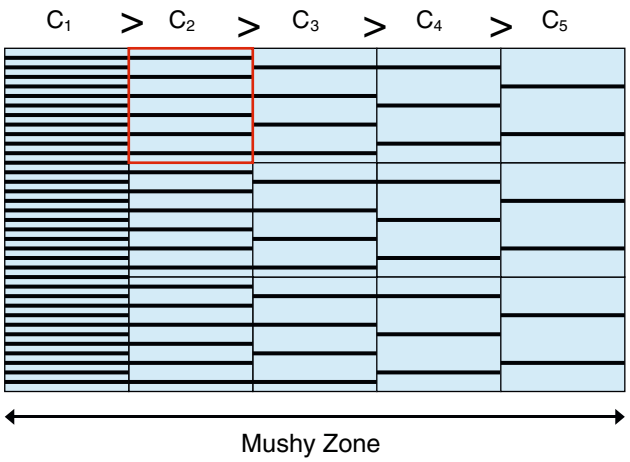

Fig. 1 A schematic showing how finite elements are visualized in a mushy zone where primary dendrite arm spacing increases with decreasing cooling rate

(moving toward the liquidus in the casting), so does the permeability of the dendritic region. The rate of change of permeability through the mushy zone is a function of the temperature profile of the mushy zone as well as the local nucleation cooling rates in this zone.

The permeability gradient model as applied in this article to the solidification of long freezing-range alloys at the final stages of freezing is examined through the following scenario:

During examination of resistance to liquid flow, dendrites are assumed to have formed a fixed structure. It is assumed that the center-to-center spacing of primary and secondary dendrites is determined during nucleation near liquidus. Cooling below this temperature affects permeability by decreasing the liquid fraction existing among the dendrite arms due to the growth of dendrites. As mentioned above, as one travels up-temperature from the frozen front of solidus, the permeability of the dendritic regions which have formed along that temperature gradient increases. That is, dendrite growth following nucleation has progressed further in locations closer to the solidification front.

Resistance to fluid flow is modeled, as in previous studies of interdendritic flow, by the D'arcy equation for average flow rate through porous media:

$$Q = \frac{KA}{\mu}\left(\frac{dP}{dx}\right) \tag{1}$$

where Q is the volumetric fluid flow rate (m^3/s) normal to the plane of solidification, K is the permeability of the porous medium (m^2), A is the cross-sectional area of the porous region (m^2), μ is the fluid's viscosity (kg/(ms)), and dP/dx (Pa/m) is the pressure differential in direction of flow across the porous medium. Summing pressure drops of all elements for the necessary flow rate gives the pressure drop across the entire permeability gradient.

The permeability of a porous medium can be determined through D'arcy's equation when values for ΔP, Q, μ, and Δx can be observed. Observation of frozen dendritic structures, noting dendrite arm spacing and liquid fraction, has also been shown to be predictive of permeability. Previous studies have modeled the porous structure of columnar dendrites as a bundle of capillary tubes.

$$Q = \frac{n\pi r^4}{8\mu}\frac{\Delta P}{L\tau}. \tag{2}$$

In the Hagen–Poisuelle treatment (Eq. 2) [4, 9], n is the number of capillaries per unit area, r is the average radius of the capillaries (m), L is the length of capillaries (m), and τ is a tortuosity factor increasing the effective length of the capillary tubes. In dendritic alloys, the capillaries in Eq. 2 are interdendritic channels. The progression from Eq. 2 to a structurally based equation for permeability (Eq. 3) derived by Santos and Melo [9] gives permeability to

interdendritic liquid flowing parallel to the primary dendrite arms (K_p). Equation 4 gives the permeability to interdendritic liquid flowing normal to the primary dendrite arms (K_n). λ_1 denotes primary dendrite arm spacing, and λ_2, secondary dendrite arm spacing. Liquid volume fraction of a given element is represented by g_L.

$$K_p = \frac{g_L^2 \lambda_1^2}{8\pi\tau^3} \tag{3}$$

and

$$K_n = \frac{g_L^2 \lambda_1 \lambda_2}{8\pi\tau^3}. \tag{4}$$

Santos and Melo [9] proposed that the tortuosity coefficient might be described by a series of the form

$$\tau = \sum_{k=0}^{i} \left(\frac{\lambda_2}{\lambda_1}\right)^{g_L^k} \tag{5}$$

which was found most predictive of experimental results for permeability for flow parallel to primary dendrite arms when $i = 3$ and for flow normal to primary dendrite arms when $i = 2$.

As the permeability of the dendritic structure depends on dendrite arm spacing and liquid fraction, dendrite arm spacing depends on cooling rate and temperature. Flemings has shown that dendrite arm spacing can be calculated from the average cooling rate during solidification of the casting, observing that primary and secondary dendrite arm spacings depend on the product of temperature gradient, G (K/m), and solidification rate, R (m/s). The product GR has the units of cooling rate (c), and experimental results are often expressed in this way. Relationship found between dendrite arm spacing and thermal variables has the form

$$\lambda = b(GR)^{-n} = bc^{-n} \tag{6}$$

where b and n are constants. Applying Eq. 6 to Eqs. 3 through 5, one may write the permeability as a function of cooling rate and liquid volume fraction in mushy zone.

Applying the model

Please note that the values at which variables were held for the evaluations (cases 1 and 2) shown below are included in Table 1.

Case 1—Unidirectional solidification of Fe–2Cr–0.5C against a constant-temperature chill block

Figure 2 shows the temperature profile of the mushy zone of a fully dendritic alloy as it cools unidirectionally. The profile is shown for three different instances. $T(t,x)$, the temperature profile employed for this case, follows the function in Eq. 7 [12], where $\alpha_s(m^2/s)$ is the thermal diffusivity of the solid structure, $T_m(K)$ is liquidus temperature, and T_0 is the temperature of a constant-temperature chill-block on one side of the mold. The boundary conditions leading to this function are uniaxial cooling, constant thermal properties, and constant chill-block temperature.

$$T(t,x) = erf\frac{x}{2\sqrt{\alpha_s t}}(T_m - T_0) + T_0 \tag{7}$$

The evaluation of the change in the element temperatures over given small time intervals establishes the basis

Table 1 Permeability gradient model inputs (*calculated)

Variable	UOM	Inputs for steel model	Inputs for aluminum model
T_m	C	1,490	647
T_s	C	1,171	557
T_0	C	20	–
$\Delta T_{superheat}$	C	100	–
$\Delta T/\Delta x$	C/m	–	1.95
c	C/s	–	–
μ	kg/m-s	0.007	0.0014
Cp	j/kg-K	2620	–
α	m^2/s	1.23E-26	–
Element length	m	1.00E-03	7.00E-04*
β		2.10E-05	3.62E-05
γ		8.00E-06	2.90E-05
n_p		0.604	0.3819
n_s		0.352	0.3258
ρ_s	kg/m^3	7,800	2,700
ρ_l	kg/m^3	7,090	2,400
$L_{casting}$	m	0.5	–

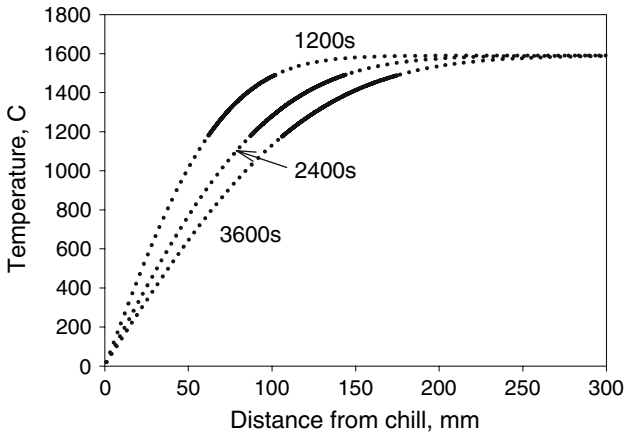

Fig. 2 Temperature profile in a steel (Fe–2Cr–0.5C) casting as it cools unidirectionally. Solid lines indicate the temperature profile in the mushy zone at a given time after the solidification begins

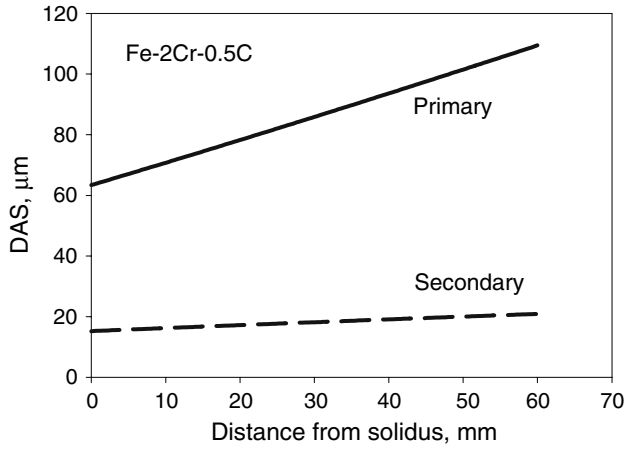

Fig. 3 Dendrite arm spacing in a mushy zone as a function of distance from solidus of the Fe–2Cr–0.5C alloy 1 h after the beginning of solidification

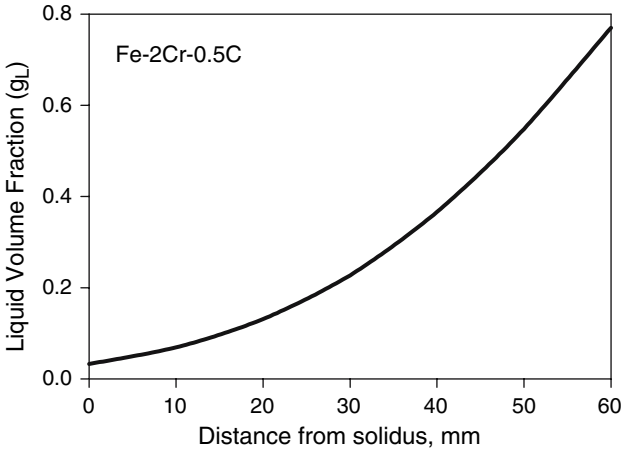

Fig. 4 Liquid volume fraction in a mushy zone as a function of distance from solidus of the Fe–2Cr–0.5C alloy

for calculating the cooling rate. Cooling rate (c) in each element is examined for two instants in time. The first is at the departure from liquidus temperature. It is assumed that this cooling rate determines the number of dendrite nuclei and therefore primary dendrite arm spacing in the cell as shown in Fig. 1. Dendrite arm spacing was determined using Eq. 6, results of which are shown in Fig. 3 for the Fe–2Cr–0.5C alloy 1 h after the beginning of solidification. The second instant of interest is immediately before a given element attains solidus temperature. The cooling rate at this second instant determines the volumetric solidification rate of the root cell. Both of these cooling rates are calculated by taking the average temperature change of each element over time intervals bracketing the instant at which the casting is being viewed.

Liquid volume fraction (g_L) is determined as a function of temperature using functions derived from a Scheil calculation performed in ThermoCalc®[1] for the modeled alloy. Distribution of liquid volume fraction in the casting is shown in Fig. 4 at 1 h after the solidification begins.

The dendrite arm spacing and liquid distribution as determined above result in a tortuosity distribution (Eq. 5) throughout the mushy zone as shown in Fig. 5a. The tortuosity parallel and normal to the orientation of the primary dendrite arms decreases with distance from the root of the solidification front at solidus. This decrease accelerates over distance due to increase in liquid volume fraction coupled with an increase in dendrite arm spacing. Figure 5b, c show the coupled effect of these variables.

Permeability of each cell is calculated using Eqs. 3 and 4. Substituting Eq. 5 for τ (tortuosity) results in a definition of permeability as a function of liquid fraction and cooling rate. The dendrite arm spacing (DAS) used in these equations is evaluated as the cell passes through liquidus. The tortuosities and resulting permeabilities in parallel and normal directions are a result of these DAS evaluations and the current liquid volume fraction. Figure 6a shows the permeability gradient existing through the mushy zone 1 h after the casting begins to solidify. This permeability gradient illustrates that the cells closest to the root of the solidification front have the greatest resistance to liquid flow. Figure 6b and c show the effect of liquid volume fraction and dendrite arm spacing on the permeability. Effect of tortuosity on the permeability (Fig. 6d) is a combination effect of dendrite arm spacing and liquid volume fraction through Eq. 5.

The controlling flow rate is determined from the volumetric freezing rate for the interdendritic fluid.

$$Q_s = \frac{V_{cell} g_L c}{\Delta T} \tag{8}$$

where Q_s is the "solid flow rate"—the rate at which the interdendritic volume (the liquid fraction) becomes filled with solid material, V_{cell} is the volume of the finite element, and ΔT is the temperature difference between the average temperature of the root cell and the alloy solidus temperature. The minimum necessary volumetric flow rate is taken as Q_s in the finite element closest to the solidus (root cell). The necessary volumetric flow rate for liquid is proportional to the minimum necessary solid volumetric flow rate by the density ratio of solid to liquid.

The required flow rate of liquid through dendritic structure results in a drop in liquid pressure across each finite element experiencing flow. This pressure drop is shown in Fig. 7. The cells closest to the solidus offer the bulk of the resistance to flow through the mushy zone (Fig. 7a). Figure 7b illustrates that the total pressure drop is very small until the solid fraction approaches 0.90.

[1] Commercial products mentioned in this paper are neither endorsed nor recommended by the USDOE. The USDOE does not endorse or recommend commercial equipment, processes, or software.

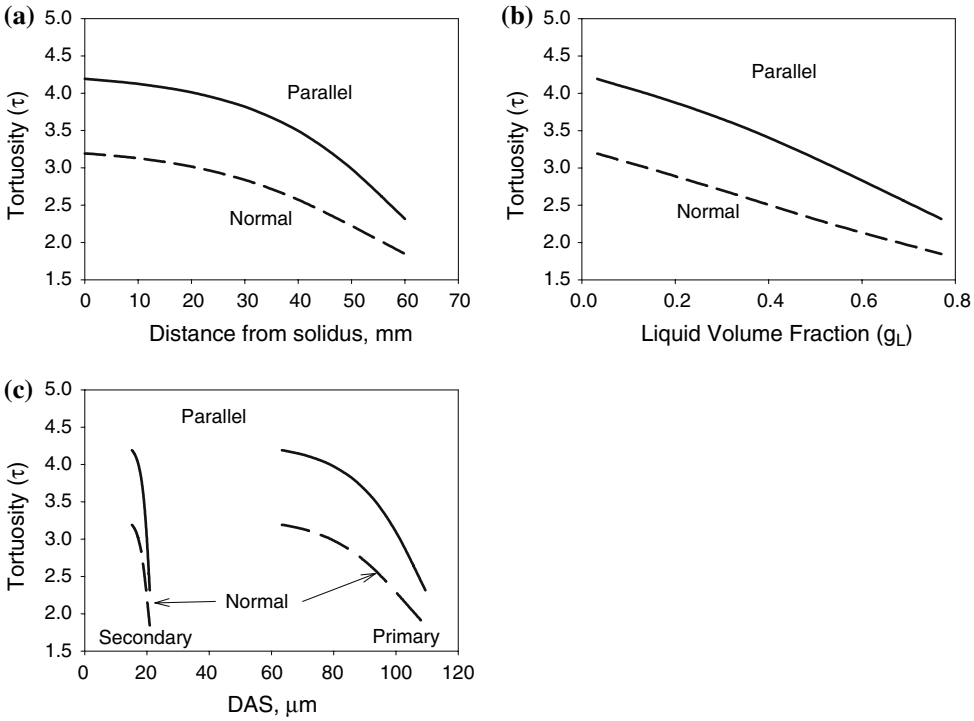

Fig. 5 Variation in tortuosity as a function of position (**a**), liquid volume fraction (**b**), and dendrite arm spacing (**c**) in a mushy zone of the Fe–2Cr–0.5C steel 1 h after solidification begins

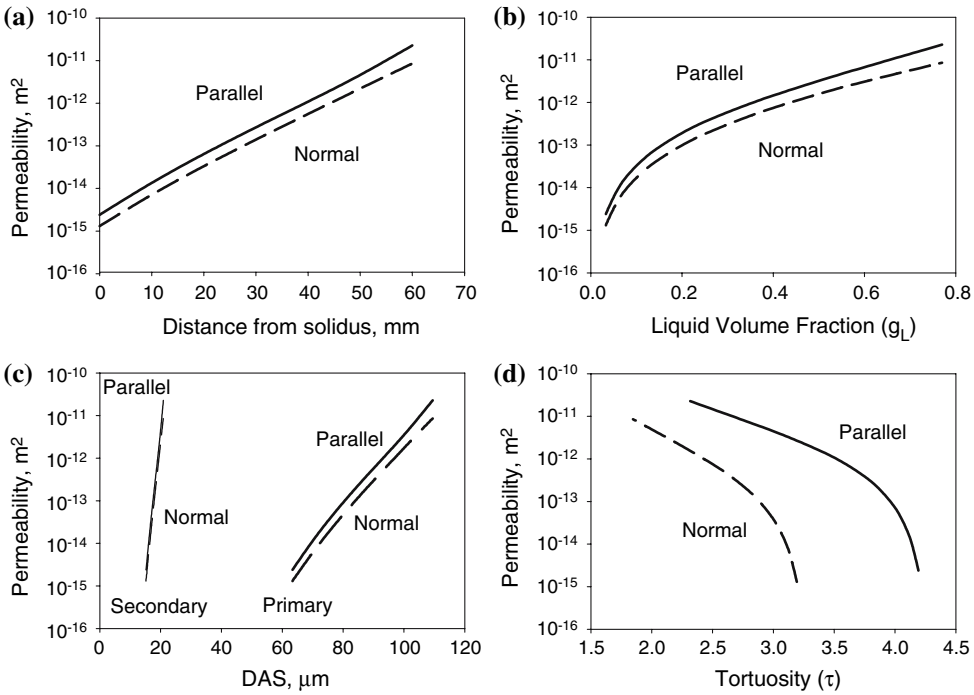

Fig. 6 Evaluation of permeability in directions parallel and normal to the primary dendrite arms as a function of position (**a**), liquid volume fraction (**b**), dendrite arm spacing (**c**), and tortuosity (**d**) in a mushy zone of the Fe–2Cr–0.5C steel 1 h after solidification begins

Thereafter, feeding liquid to the root cell requires a significant increase in the driving pressure.

This model provides a prediction of the minimum head pressure required at the liquid end of the mushy zone to ensure complete and timely feeding of the root cell. If the head pressure is less than the total pressure drop across all the elements of the mushy zone, porosity is predicted.

Case 2—Unidirectional solidification of Al–5Cu in a linear temperature gradient

The permeability gradient model is applied to the data given by Horwath and Mondolfo [14] for Al–5%Cu. In their study, the temperature gradient was recorded as 2.7 K/cm throughout the casting. The cooling rate was 0.18 K/s. From

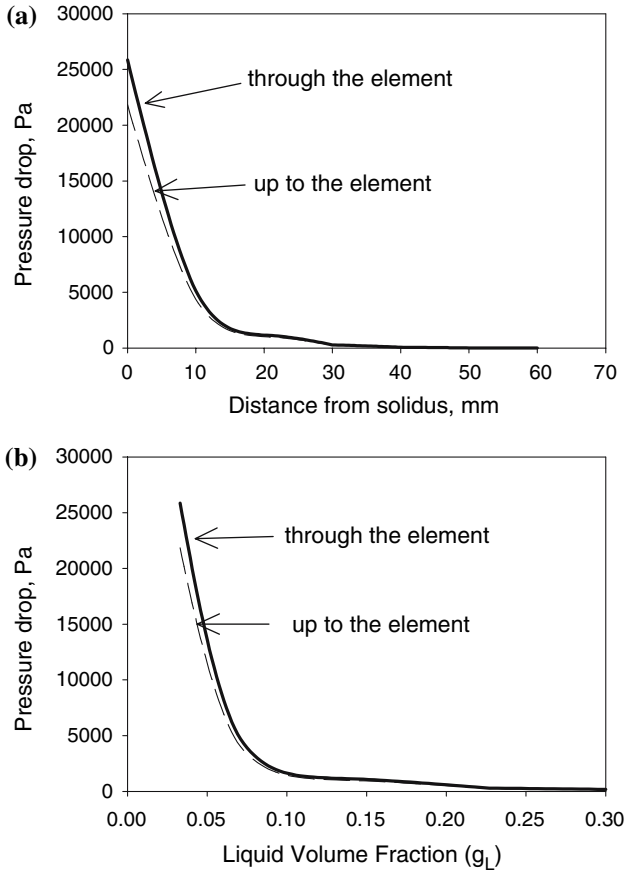

Fig. 7 Evaluation of pressure drop in liquid as a function of position (**a**) and liquid volume fraction (**b**) in a mushy zone of the Fe–2Cr–0.5C steel 1 h after solidification begins

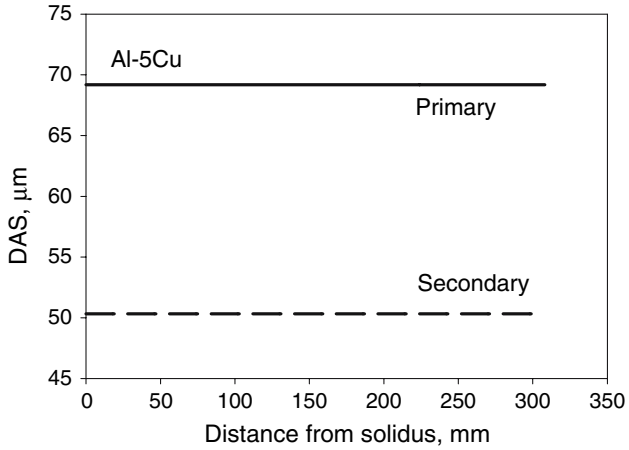

Fig. 8 Dendrite arm spacing in a mushy zone as a function of distance from solidus of the Al–5Cu alloy 1 h after the beginning of solidification

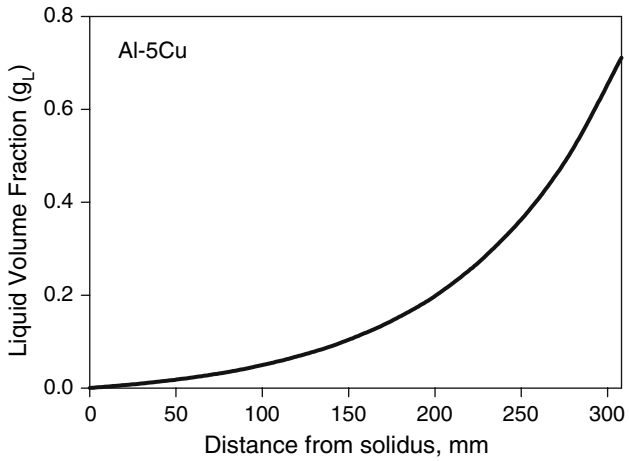

Fig. 9 Liquid volume fraction in a mushy zone as a function of distance from solidus of the Al–5Cu alloy

these data, mushy zone length was calculated as 33 cm. Dendrite arm spacing was evaluated using Eq. 6. Primary DAS (Dendrite Arm Spacing) as 69 µm while secondary DAS was 50 µm. These dendrite arm spacings were constant throughout the mushy zone at all times (Fig. 8).

Liquid volume fraction was calculated as a function of temperature using ThermoCalc® software. This is plotted in Fig. 9 as a function of distance from solidus. Tortuosity is plotted as a function of distance from solidus and of liquid volume fraction in Fig. 10. Since the DAS is constant throughout the mushy zone in Al–5Cu, the change in tortuosity is due only to liquid volume fraction. In both parallel and normal flow directions, this change is modest. It follows that the more dramatic tortuosity change in the steel case (Fig. 5a) is dominated by the change in dendrite arm spacing.

Permeability of dendritic structure in the Al–5Cu case is shown in Fig. 11 as a function of distance from solidus, liquid volume fraction, and tortuosity. Permeabilities of the cells near solidus drop sharply several orders of magnitude. Although this sharp drop is not observed in the steel example, the difference can be explained by the fact that the minimum liquid volume fraction examined in the steel case was about 0.04 whereas the minimum liquid volume fraction examined in the Al–5Cu case was actually zero.

The other difference between the permeabilities of the steel and the Al–5Cu is relative magnitude of permeabilities in parallel and normal directions. While the permeability in the parallel direction is higher in the steel case than in the normal direction, it is lower than the normal direction in the Al–5Cu case. This difference is due to the fact that in the steel case the secondary DAS is much smaller than the primary DAS whereas in the Al–5Cu case, the secondary and the primary DAS are much more similar. Examining Eqs. 3 and 4, it becomes evident that this difference between primary and secondary DAS results in the descriptive equations being dominated by the numerator which describes cross-sectional area of the flow channel. The same difference between the primary and secondary

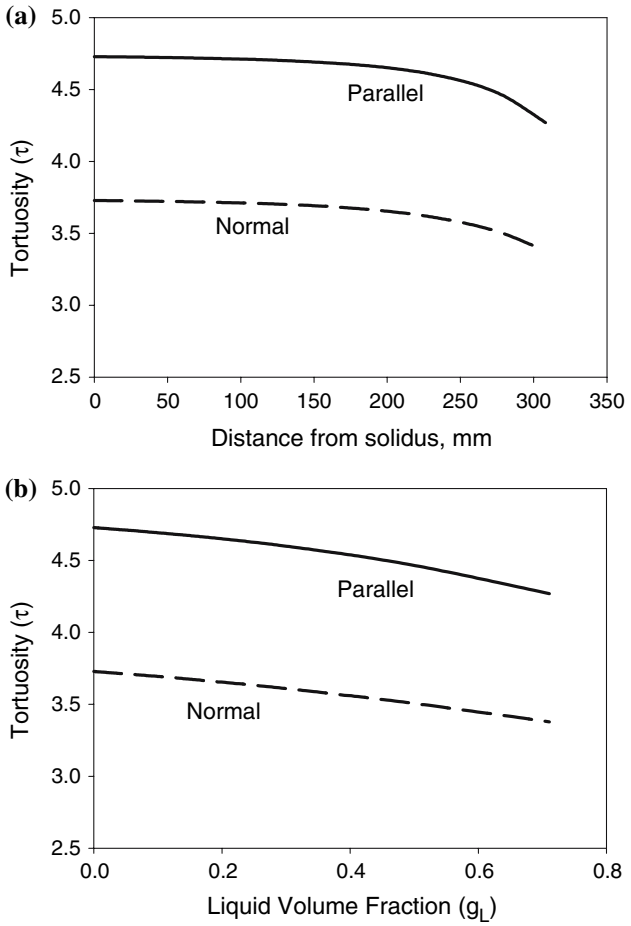

Fig. 10 Variation in tortuosity as a function of position (**a**) and liquid volume fraction (**b**) in a mushy zone of the Al–5Cu alloy 1 h after solidification begins

DAS does not change the fact that tortuosity in the parallel direction is always higher than the normal direction as shown in Figs. 5 and 10.

In Figs. 7a and 12a, the pressure drop plotted is the total pressure drop from liquidus up to and through a given cell in the mushy zone in the Fe–2Cr–0.5C alloy and the Al–5Cu alloy, respectively. The pressure drop across the mushy zone of Al–5Cu is much higher than that found in the steel case. Both cases show insignificant pressure drop at 30 mm from the solidus. The change in total pressure drop with distance and liquid volume fraction is greater in the Al–5Cu case. The primary reason that the total pressure drop is much smaller in the steel case is the fact that, in the steel case, the dendritic solidification stops at a liquid volume fraction of 0.04 whereas dendritic solidification of Al–5Cu is carried through a liquid volume fraction of zero. The primary reason for the greater change in the Al–5Cu case lies in the fact that even the most permeable cell (that contributing least to the pressure drop) in the Al–5Cu case (Fig. 12a) is less permeable than the root cell (closest to solidus) in the steel case (Fig. 7a).

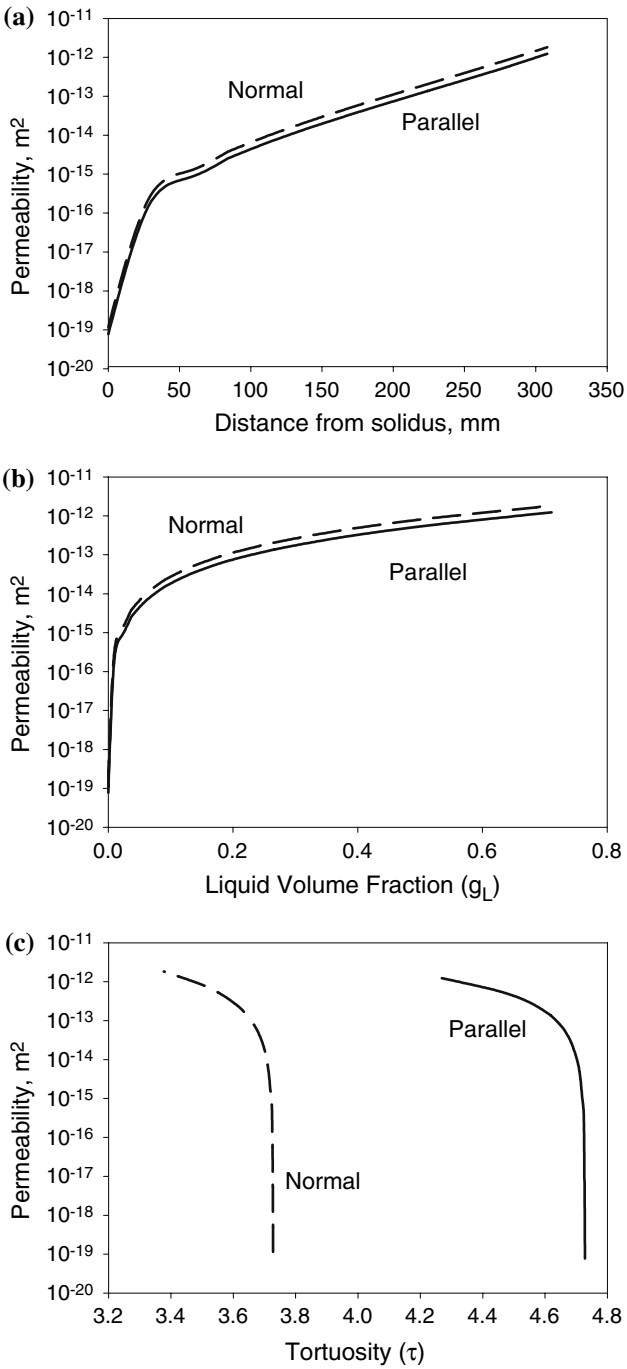

Fig. 11 Evaluation of permeability in directions parallel and normal to the primary dendrite arms as a function of position (**a**), liquid volume fraction (**b**), and tortuosity (**c**) in a mushy zone of the Al–5Cu alloy 1 h after solidification begins

Conclusions

A fluid flow model based on a permeability gradient in mushy zone of dendritically freezing alloys was presented, addressing interstitial tortuosity, permeability, and liquid pressure-drop as a function of permeability and required

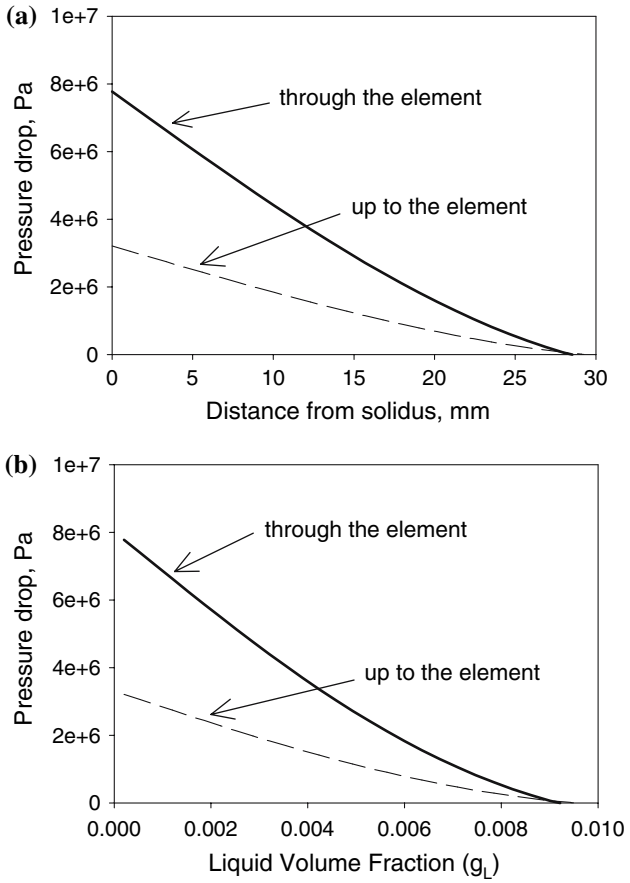

Fig. 12 Evaluation of pressure drop in liquid as a function of position (**a**) and liquid volume fraction (**b**) in a mushy zone of the Al–5Cu alloy 1 h after solidification begins

feeding rate for shrinkage-porosity prevention. Application of the model to two different solidification cases was shown. Tortuosity, permeability, and resulting pressure drop across a mushy zone were examined for a steel freezing unidirectionally against a chill block at a constant temperature and an aluminum alloy solidifying unidirectionally in a linear temperature gradient. Tortuosity of a dendritic mushy zone depends on both liquid volume fraction and dendritic arm spacing. The dendritic arm spacing has a much stronger effect on tortuosity than the liquid volume fraction. Permeability of a dendritic structure is a strong function of both liquid fraction and dendrite arm spacing. As the ratio of primary to secondary DAS becomes larger, the dendritic structure becomes more permeable in the flow direction parallel to primary arms for a given liquid volume fraction. Greatest resistance to liquid feeding within the mushy zone occurs near the root of the solidification front (solidus). Presence of even a small amount of eutectic liquid near the root of the solidification front increases the permeability dramatically.

Acknowledgement This report based upon work supported by the U.S. Department of Energy under Award Number DE-FC36-01ID13981.

References

1. Geiger GH, Poirier DR (1973) Transport phenomena in metallurgy. Addison-Wesley, Reading, p 91
2. Geiger GH, Poirier DR (1973) Transport phenomena in metallurgy. Addison-Wesley, Reading, p 45
3. Duncan AJ, Han Q, Viswanathan S (1999) Metall Mater Trans B 30B:745
4. Streat N, Weinberg F (1976) Interdendritic fluid flow in a lead–tin alloy. Metall Trans B 7B:417
5. Murakami K, Shiraishi A, Okamoto T (1983) Interdendritic fluid flow normal to primary dendrite-arms in cubic alloys. Acta Metall 31(9):1417
6. Nielsen O, Arnberg L, Mo A, Thevik H (1999) Experimental determination of mushy zone permeability in aluminum–copper alloys with equiaxed microstructures. Metall Mater Trans A 30A:2455
7. Wang CY, Ahuja S, Beckermann C, de Groh III HC (1995) Metall Mater Trans B 26B:111
8. Nasser-Rafi R, Desmunkh R, Poirier DR (1985) Flow of interdendritic liquid and permeability in Pb-20 Wt Pct Sn alloys. Metall Trans A 16A:2263
9. Santos RG, Melo MLNM (2005) Permeability of interdendritic channels. Mater Sci Eng A 391:151
10. Sabau AS, Viswanathan S (2002) Microporosity in aluminum alloy casting. Metall Mater Trans B 33B:243
11. Niyama E, Uchida T, Morikawa M, Saito S (1982) A method of shrinkage prediction and its application to steel casting practice. AFS International Cast Metals Journal, pp 52–63
12. Flemings MC (1974) Solidification processing, materials science and engineering series. McGraw-Hill, New York, NY, p 148
13. Bejan A, Dincer I, Lorente S, Miguel A, Reis H (2004) Porous and complex flow structures in modern technologies. Springer-Verlag, New York, p 10
14. Horwath JA, Mondolfo LF (1962) Dendritic growth. Acta Metall 10:1037